Int J Thermophys (2010) 31:831–843
DOI 10.1007/s10765-010-0739-3

The Transport Properties of Sodium Atoms and the Heat Capacity of Sodium Dimers at High Temperatures

L. Biolsi · P. M. Holland

Received: 16 June 2009 / Accepted: 2 April 2010 / Published online: 21 April 2010

Abstract Including the contribution of excited state atoms can improve calculations of dilute gaseous transport properties at high temperatures. For sodium, experimental and/or theoretical information is available about the potential energy curves associated with each of ten low-lying states of the sodium dimer. These include the $X^1\Sigma_g{}^+$ and $^3\Sigma_u{}^+$ states that dissociate to two ground state ^{2}S sodium atoms and the four $^3\Sigma_{g,u}{}^+$, $^1\Sigma_{g,u}{}^+$, $^1\Pi_{g,u}$, $^3\Pi_{g,u}$ gerade/ungerade pairs of states that dissociate to a ground state ^{2}S atom and an excited state ^{2}P atom. Nine of these are bound states and have been fitted with the Hulburt–Hirschfelder potential, a very good general purpose atom–atom potential. The $^3\Pi_g$ state is not bound and has been fitted with the exponential repulsive potential. We have used these potentials to calculate viscosity collision integrals as a function of temperature, and employed degeneracy-weighted averaging to determine the viscosity and translational contribution to the thermal conductivity of the sodium atoms. These same potentials have been used to calculate the heat capacity, C_p^o, of the sodium dimer using an approach that depends on the second virial coefficient and its first two temperature derivatives. Again, the inclusion of molecular states that dissociate to an excited state atom allows C_p^o to be determined with improved accuracy at higher temperatures. Thus, thermophysical property calculations for sodium have been extended to 25,000 K. These results are compared with previous results, including heat capacities given in the *NIST-JANAF Thermochemical Tables*.

Keywords Heat capacity · Sodium · Thermal conductivity · Viscosity

L. Biolsi (✉)
Chemistry Department, Missouri University of Science and Technology, Rolla, MO 65401, USA
e-mail: biolsi@mst.edu; louis@biolsi.com

P. M. Holland
Thorleaf Research, Inc., 5552 Cathedral Oaks Road, Santa Barbara, CA 93111-1406, USA

1 Introduction

Various calculations are available for the transport properties [1–3] and the second virial coefficients [3–5] of monatomic sodium, Na, and the heat capacity [6] of the sodium dimer, Na_2. This previous work involved the consideration of either the ground $X^1\Sigma_g^+$ (1) state potential energy curve of Na_2 only, or this state and the other potential energy curve that dissociates to two ground state ^{2}S sodium atoms, the weakly bound $^3\Sigma_u^+$ (1) state. The purpose of the present work is to also include Na_2 states that dissociate to one ground state ^{2}S atom and one first excited state ^{2}P atom, so that the viscosity and translational thermal conductivity of sodium atoms and the heat capacity of the sodium dimer can be accurately calculated to significantly higher temperatures.

When a ^{2}S and a ^{2}P atom interact, they can follow any of eight potential energy curves, those corresponding to the $^1\Sigma_u^+$, $^3\Sigma_g^+$, $^1\Sigma_g^+(2)$, $^3\Pi_u$, $^1\Pi_u$, $^1\Pi_g$, $^3\Sigma_u^+(2)$, and $^3\Pi_g$ states of the dimer [7]. The symbols (1) and (2) are used to distinguish between states with the same term symbol. These ten states are included in the present thermophysical property calculations. Nine of the states are bound, but the $^3\Pi_g$ state is repulsive.

2 Potential Energy Curves

The Hulburt–Hirschfelder (HH) potential is a very good general purpose atom–atom potential for representing interactions with an attractive minimum in the potential [8–12]. Indeed, it may represent the true potential better [13] than the representation provided by the "experimental" Rydberg–Klein–Rees [14–16] (RKR) potential. For example, it is capable of representing double minima arising from avoided curve crossings [13,17–19]. This potential has been discussed in detail elsewhere [18,20, 21].

The HH potential is a spectroscopic potential, and it is completely determined by the experimental spectroscopic constants for an electronic state of a diatomic molecule. Alternatively, it can be used to accurately fit theoretical potential energy curves. The HH potential is used to represent the nine attractive potential energy curves of Na_2 considered here.

Experimental spectroscopic constants are available for seven states: the $X^1\Sigma_g^+$ (1) [22], $^3\Sigma_u^+$ (1) [23], $^1\Sigma_u^+$ [6], $^3\Pi_u$ [24], $^1\Sigma_g^+$ (2) [25], $^1\Pi_g$ [25], and $^1\Pi_u$ [22,26] states. The HH potentials have been determined directly from the spectroscopic constants for these states. Theoretical potential energy curves are available for the $^3\Sigma_g^+$ and $^3\Pi_g$ states [27] and for the $^3\Sigma_u^+$ (2) state [28]. The bound $^3\Sigma_g^+$ and $^3\Sigma_u^+$ (2) states were fit with the HH potential, and the $^3\Pi_g$ state was fit with the exponential repulsive potential. Fits for these three states are shown in Fig. 1. The fit is excellent for the $^3\Sigma_g^+$ state but quite poor for the other two states at larger values of r, the interatomic separation. However, as discussed later, this should have very little effect on the accuracy of the results.

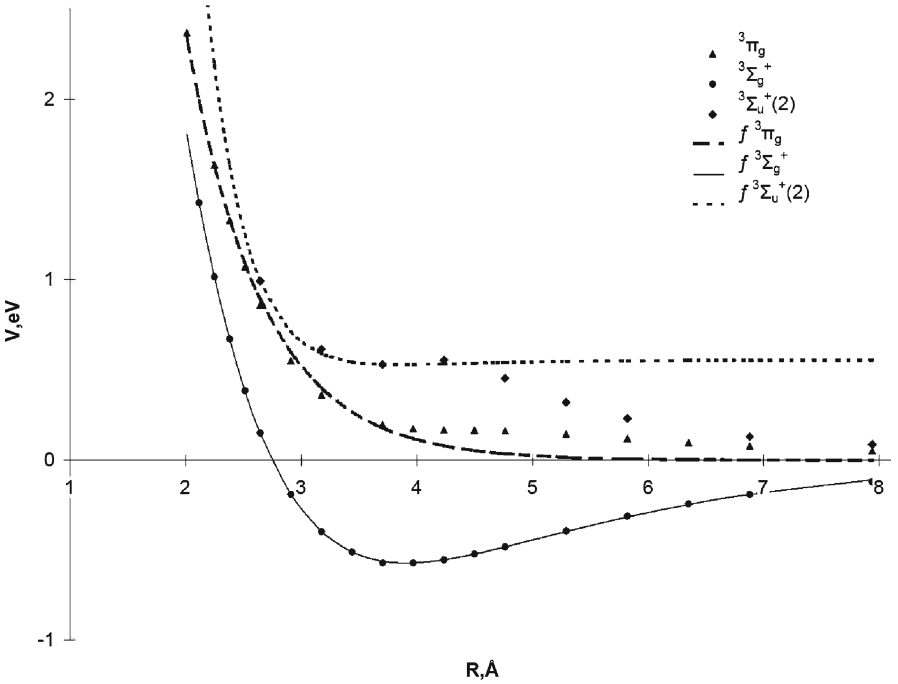

Fig. 1 Comparison of the theoretical results [27,28] for three electronic states of Na_2 with the fitted potentials for these states. Zero of energy is taken to be the separated $^1S + ^2P$ atoms

3 Heat Capacity of Na_2

The heat capacity of Na_2 is calculated using a method based on virial coefficients [29]. The heat capacity, C_p^o, is given by [30,31]

$$C_p^o = R\left[4 + 2\frac{B_1^*(T^*)}{B^*(T^*)} + \frac{B_2^*(T^*)}{B^*(T^*)} - \left(\frac{B_1^*(T^*)}{B^*(T^*)}\right)^2\right] \tag{1}$$

where R is the universal gas constant, B^* is the second virial coefficient in reduced units, T^* is the reduced temperature, and B_1^* and B_2^* are essentially the reduced first and second derivatives, respectively, of the second virial coefficient. These reduced quantities are given by

$$T^* = \frac{kT}{D_e} \quad B^*(T^*) = \frac{B(T)}{b_o} \tag{2}$$

$$B_1^*(T^*) = T^*\left(\frac{dB^*}{dT^*}\right) \quad B_2^*(T^*) = (T^*)^2\left(\frac{d^2B^*}{dT^{*2}}\right) \tag{3}$$

where k is Boltzmann's constant, T is the temperature in K, D_e is the electronic dissociation energy, b_o is the rigid sphere second virial coefficient for the molecule, i.e., [32],

$$b_o = \frac{2\Pi}{3}\sigma^3 \tag{4}$$

where σ is the effective rigid sphere diameter for the molecule, taken to be the smallest value of r at which the potential energy is zero, and $B(T)$ is the virial coefficient, in $m^3 \cdot mol^{-1}$.

At high temperatures, there is a contribution to the virial coefficient from a variety of electronic states, labeled i, of the molecule. The final result for the virial coefficient is obtained by averaging over the degeneracy of each state (degeneracy averaging) [4], i.e.,

$$B^*(T^*)_{av} = \frac{\sum_i B_i^*(T^*) g_i(\mathrm{Na_2}) e^{-E_i(\mathrm{Na_2})/kT}}{\left(\sum_j g_j(\mathrm{Na}) e^{-E_j(\mathrm{Na})/kT}\right)^2} \tag{5}$$

where g_i and E_i represent the degeneracy and energy, respectively, of Na_2 in electronic state i and g_j and E_j represent the degeneracy and energy, respectively, of Na in electronic state j. There are similar expressions for the first and second derivatives of $B^*(T^*)_{av}$.

The classical expression for the virial coefficient in electronic state i, $B_{cl,i}(T)$, is given by [32]

$$B_{cl,i}(T) = 2\Pi N_o \int_0^\infty \left(1 - e^{-V_i(r)/kT}\right) r^2 dr \tag{6}$$

where N_o is Avogadro's number and $V_i(r)$ represents the potential energy curve for the molecule in state i as a function of interatomic separation. The first three semi-classical expressions for $B_i(T)$ are also included in the calculation. These somewhat lengthy results, which depend on the derivatives of $V_i(r)$ with respect to r, are given elsewhere [32–34]. Thus, the virial coefficient for an electronic state depends only on the potential energy for that state; in this case it is determined by the nine bound state potentials of Na_2 discussed above.

The second virial coefficient and its derivatives are calculated for each state using the HH potential in Eq. 6 to represent the electronic interaction. The HH potential, $V_{HH,i}(r)$, is given by [20,21]

$$\begin{aligned} V^*_{HH,i}(r_i^*) = {} & e^{-2A_i(r_i^*/d_i - 1)} - 2e^{-A_i(r_i^*/d_i - 1)} \\ & + B_i(r_i^*/d_i - 1)^3 \left[1 + G_i\left(r_i^*/d_i - 1\right)\right] e^{-2A_i(r_i^*/d_i - 1)} \end{aligned} \tag{7}$$

in reduced units, where

$$V^*_{HH,i} = \frac{V_{HH,i}}{D_{e,i}} \quad r_i^* = \frac{r}{\sigma_i} \quad d_i = \frac{r_{e,i}}{\sigma_i}$$

and $V_{\mathrm{HH,i}}$ is the HH potential for electronic state i and $r_{\mathrm{e},i}$ is the position of the minimum in the potential for the molecule in electronic state i. Also,

$$A_i = \frac{\omega_{\mathrm{e},i}}{\sqrt{2B_{\mathrm{e},i}D_{\mathrm{e},i}}} \qquad B_i = c_i A_i^3 \qquad G_i = b_i A_i$$

$$c_i = 1 + a_{1,i}\sqrt{\frac{D_{\mathrm{e},i}}{a_{0,i}}} \qquad b_i = 2 - \frac{7/12 - D_{\mathrm{e},i}a_{2,i}/a_{0,i}}{c_i}$$

and

$$a_{0,i} = \frac{\omega_{\mathrm{e},i}^2}{4B_{\mathrm{e},i}} \quad a_{1,i} = -1 - \frac{\alpha_{\mathrm{e},i}\omega_{\mathrm{e},i}}{6B_{\mathrm{e},i}^2} \quad a_{2,i} = \frac{5a_{1,i}^2}{4} - \frac{2\omega_{\mathrm{e}}\chi_{\mathrm{e},i}}{3B_{\mathrm{e},i}}$$

In addition, $\omega_{\mathrm{e},i}$ is the fundamental vibrational frequency, $\omega_{\mathrm{e}}\chi_{\mathrm{e},i}$ is the anharmonicity constant, $B_{\mathrm{e},i}$ is the rotational constant, and $\alpha_{\mathrm{e},i}$ is the rotation–vibration coupling constant. These are the spectroscopic constants for the Na_2 molecule in electronic state i. The HH potential depends on these constants and the constants $D_{\mathrm{e},i}$ and $r_{\mathrm{e},i}$. These six constants are known experimentally for seven of the nine states of Na_2 that contribute to the heat capacity. Theoretical results for the other two bound states were fit with the HH potential to find A_i, B_i, and G_i.

The results we calculated for C_p^{o} as a function of temperature using this procedure are shown in the second column of Table 1, the fractional contributions of the different states of Na_2 to $B^*(T^*)_{\mathrm{av}}$ are shown in Table 2, and the Boltzmann factors for the dissociated sodium atoms are shown in Table 3.

The results for the heat capacity of Na_2 as a function of temperature given in the *NIST-JANAF Thermochemical Tables* [6] are shown in the third column of Table 1. The method used to generate the data in this table is based on the usual expression for the partition function, q, of a diatomic molecule [6];

$$q = q_{\mathrm{tr}}q_{\mathrm{int}} \tag{8}$$

where q_{tr} is the translational contribution to the partition function and q_{int}, the internal contribution to the partition function, is written as a sum over electronic states, i, with a vibrational–rotational contribution from each electronic state;

$$q_{\mathrm{int}} = \sum_i \left(g_i \mathrm{e}^{-E_i/kT} \sum_{v_i, J_i} g(v_i, J_i)\mathrm{e}^{-E(v_i,J_i)/kT} \right) \tag{9}$$

where g_i is the electronic degeneracy, E_i is the electronic energy, and v_i and J_i are the vibrational and rotational quantum numbers, respectively, in electronic state i. Also $g(v_i, J_i)$ represents the vibrational and rotational degeneracies and $E(v_i, J_i)$ is the vibrational–rotational energy, given by

Table 1 Heat capacity, $C_p^o(\mathrm{J \cdot mol^{-1} \cdot K^{-1}})$ of Na_2 as a function of temperature

T (K)	All[a]	Ref. [6][b]	Ref. [6], also[c]	$^2S + {}^2S$[d]
298.15	37.79	37.58	37.78	37.79
500	38.46	38.33	38.44	38.46
1000	40.54	39.37	40.59	40.54
1500	39.12	36.55	39.85	39.23
2000	35.16	32.78	35.33	35.13
2500	31.78	31.70	33.04	31.64
3000	29.52	34.60	30.72	29.17
3500	28.09	40.67	29.20	27.46
4000	27.19	47.43	28.21	26.26
4500	26.57	52.30	27.54	25.36
5000	26.14	54.05	27.07	24.67
6000	25.54	50.11	26.41	23.65
7000	25.16		25.97	22.90
8000	24.89		25.66	22.27
9000	24.69		25.43	21.72
10000	24.54		25.26	21.21
12500	24.29		24.99	19.19
15000	24.13		24.84	18.75
17500	24.02		24.74	17.43
20000	23.94		24.68	15.98

[a] Virial coefficient results using the $X^1\Sigma_g^+$ (1), $^3\Sigma_u^+$ (1), $^1\Sigma_u^+$, $^3\Sigma_g^+$, $^1\Sigma_g^+$ (2), $^3\Pi_u$, $^1\Pi_u$, $^1\Pi_g$, and $^3\Sigma_u^+$ (2) states of Na_2

[b] Partition function results from Ref. [6]

[c] Virial coefficient results obtained by us using the same electronic states used in Ref. [6]

[d] Virial coefficient results using only the two states of Na_2, the $X^1\Sigma_g^+$ (1) and $^3\Sigma_u^+$ (1) states, that dissociate to two ground state ^2S atoms

Table 2 Fractional contribution of each electronic state of Na_2 to $B^*(T^*)_{av}$ as a function of temperature

T (K)	$X^1\Sigma_g^+$ (1)	$^3\Sigma_u^+$ (1)	$^1\Sigma_u^+$	$^3\Sigma_g^+$	$^1\Sigma_g^+$ (2)	$^3\Pi_u$	$^1\Pi_u$	$^1\Pi_g$	$^3\Sigma_u^+$ (2)
298.15	1.00								
1000	1.00								
2500	0.99	.01							
3000	.97	.01				.01			
5000	.74	.03	.03	.02		.18			
10000	.24	.03	.08	.08		.55		.01	
15000	.13	.02	.10	.09	.01	.63		.01	
20000	.09	.02	.11	.10		.66		.01	.01

$$E(v_i, J_i) = \omega_{e,i}(v_i + 1/2) - \omega_e\chi_{e,i}(v_i + 1/2)^2 + B_{e,i}J_i(J_i + 1) - D_i J_i^2(J_i + 1)^2 - \alpha_{e,i}(v_i + 1/2)J_i(J_i + 1) \quad (10)$$

where $\omega_{e,i}$, $\omega_e\chi_{e,i}$, $B_{e,i}$, and $\alpha_{e,i}$ are the spectroscopic constants referred to previously and D_i is the centrifugal stretching spectroscopic constant.

Table 3 Boltzmann factors for the dissociated Na atoms

T (K)	$^1S + {}^1S$	$^1S + {}^2P$	$^2P + {}^2P$
500	1.00		
1000	1.00		
5000	1.00	0.01	
10000	1.00	0.08	0.01
15000	1.00	0.18	0.03
20000	1.00	0.28	0.08
25000	1.00	0.36	0.13

Both the Woolley approach [29] and the Chase approach [6] depend on the spectroscopic constants. Of course, they are related, but they involve quite different calculational procedures. We will refer to the Woolley approach [29] as the "virial approach" and to the Chase approach [6] as the "state sum approach."

4 Viscosity and Thermal Conductivity of Na

The viscosity, η, of a monatomic gas is given by [32]

$$\eta(\mu\text{Pa}\cdot\text{s}) = 2.669\frac{\sqrt{MT}}{\sigma^2\Omega^{(2,2)^*}} \tag{11}$$

and the translational contribution to the thermal conductivity, λ_{tr}, of a monatomic gas is given by [32]

$$\lambda_{\text{tr}}(\text{W}\cdot\text{m}^{-1}\cdot\text{K}^{-1}) = 0.08322\frac{\sqrt{T/M}}{\sigma^2\Omega^{(2,2)^*}} \tag{12}$$

where T is the temperature in K, M is the molar mass in $\text{g}\cdot\text{mol}^{-1}$, and $\sigma^2\Omega^{(2,2)^*}$ is the viscosity collision integral, involving elastic collisions, in $10^{-20}\,\text{m}^2$. The degeneracy-averaged viscosity collision integral is expressed by [35,36]

$$\sigma^2\Omega_{\text{da}}^{(2,2)^*} = \sum_i \alpha_i \sigma_i^2 \Omega_i^{(2,2)^*} \text{e}^{-E_i/kT} \tag{13}$$

where, again, i represents the electronic state and E_i is the energy of the separated atoms corresponding to that state. The quantity α_i represents the probability of each state, i.e., for the two states that dissociate to ground state atoms, α_i is 1/4 for the $X^1\Sigma_g^+$ (1) state and 3/4 for the $^3\Sigma_u^+$ (1) state. The Boltzmann factor assumes that there is an equilibrium composition of states, which is a reasonable assumption, since the transport properties are near-equilibrium properties. The transport properties that we have calculated using this approach are shown in Table 4. A program that calculates transport properties for the HH potential [18] was used for the nine bound states and

Table 4 Viscosity, η, and translational contribution to the thermal conductivity, λ_{tr}, as a function of temperature

T (K)	$\eta(\mu\text{Pa} \cdot \text{s})$	$\lambda_{tr}(\text{W} \cdot \text{m}^{-1} \cdot \text{K}^{-1})$
500	10.25	0.01391
750	14.54	0.01972
1000	18.32	0.02484
1250	21.75	0.02949
1500	24.99	0.03390
2000	31.29	0.04244
2500	37.61	0.05100
3000	44.00	0.05968
3500	50.46	0.06844
4000	56.86	0.07712
4500	63.22	0.08574
5000	69.42	0.09415
6000	81.27	0.1102
7000	92.28	0.1251
8000	102.5	0.1390
9000	112.0	0.1519
10000	120.9	0.1640
12500	141.3	0.1917
15000	159.9	0.2169
17500	177.4	0.2406
20000	194.2	0.2633

tabulations of collision integrals for the exponential repulsive potential [37] were used for the $^3\Pi_g$ state.

5 Discussion

Our calculated "virial approach" results for C_p^o using nine states of Na_2, shown in column 2 of Table 1, can be compared to the "state sum approach" results from the *NIST-JANAF Thermochemical Tables* [6], shown in column 3. In addition, virial results calculated by us using the same states used to obtain the state sum results in Ref. [6], are shown in column 4. Finally, virial results we obtain when we include only the two Na_2 states that dissociate to ground state ^{2}S atoms are shown in column 5 of Table 1.

Each of our virial calculations shows that C_p^o reaches a maximum between 900 K and 1200 K, and then decreases. However, the state sum results in Ref. [6] show that C_p^o rises to a maximum near 1000 K and then decreases to a "local" minimum at about 2500 K and, finally, rapidly increases to 6000 K, the highest temperature considered in that calculation. None of our calculations exhibit this behavior and, instead, show C_p^o decreasing steadily after reaching its maximum value as the temperature increases

to 20,000 K. Also, at 6000 K the *NIST-JANAF* result [6] for C_p^o is approximately twice as large as any result we obtain using the virial approach.

The behavior shown for Na_2 in Ref. [6], in which C_p^o goes through a maximum and then decreases to a minimum before increasing again, is rather unusual. Those calculations do not include the first excited $^3\Sigma_u^+$ (1) state and the eight bound states that dissociate to ^{2}S and ^{2}P atoms are represented by using only the $^1\Sigma_u^+$ state and a degeneracy of 10 to qualitatively represent the $^3\Sigma_g^+$ and $^3\Pi_u$ states. Table 2 shows the fractional contribution of each electronic state to $B^*(T^*)_{av}$ as a function of temperature. At 2500 K, where the *NIST-JANAF* results for C_p^o reach a minimum, the $^3\Sigma_u^+$ (1) state begins to make a contribution. At about 5000 K, the states that dissociate to an excited atom begin to make significant contributions that increase as the temperature increases. Table 2 also shows that the $^3\Sigma_g^+$ state, not specifically included in the *NIST-JANAF* calculations, contributes about as much to C_p^o as the $^1\Sigma_u^+$ state included in those calculations and the $^3\Pi_u$ state, also not specifically included in the *NIST-JANAF* calculations, makes the largest contribution at higher temperatures. Although the same behavior shown for Na_2 is also shown in the *NIST-JANAF* tables [6] for Li_2 and Cs_2, but not for K_2 or Rb_2, the comment is made [6] that "deficiencies" and "problems" occur for C_p^o above 2000 K due to the approximations made for excited states. Thus, we think it is unlikely that the behavior of C_p^o at high temperatures for Na_2 given in Ref. [6] is correct.

Columns 2 and 5 of Table 1 give nearly the same results for C_p^o below about 10,000 K when excited states begin to contribute significantly to thermodynamic properties.

Both methods for calculating C_p^o depend on the spectroscopic constants; the virial approach as augmented here by using the spectroscopically determined HH potential in Eq. 7, and the state sum approach through Eq. 10. There are a number of potential errors associated with the state sum approach as one goes to higher temperatures. The spectroscopic constants in the expression for the vibrational–rotational energy, Eq. 10, are obtained by making a fit to infrared spectra in such a way that the fit becomes less accurate as the quantum numbers v_i and J_i increase [4,30,34,38,39]. Since vibrational states become very closely spaced as v_i becomes large, the high density of high v_i states makes this contribution significant [4]. Also, the term in $(V_i + 1/2)^2$ in Eq. 10 diverges as v_i becomes large [4].

In addition, the state sum approach does not usually include a contribution to C_p^o from the continuum states (corresponding to the repulsive part of the potential). This is the case [6] for Na_2. We have shown [40] that, using the virial approach, erroneous results for C_p^o for Ag_2 are obtained if the repulsive part of the potential is ignored. For Na_2, at 2500 K, where the *NIST-JANAF* results differ from our results by less than 0.2 %, a recalculation of C_p^o using the virial approach but ignoring the repulsive part of the potential, gives the result, $C_p^o = 25.43\,\mathrm{J \cdot mol^{-1} \cdot K^{-1}}$, a difference of 20 % from the results in the second and third columns of Table 1.

There are, of course, also errors in the virial approach, mostly due to errors in the potential used to represent the atom–atom interactions; in this case, the HH potential. Table I and Fig. 1 in Ref. [3] indicate that the spectroscopically determined HH potential for the ground state gives good agreement with the "experimental" RKR potential [2] for this state except along the repulsive part of the potential. In general, one would

expect any spectroscopically determined potential, such as the HH potential, to give the best fit to the "true" (e.g., RKR) potential in the well region which is the region that dominates in the determination of the spectroscopic constants. The fit is expected to be poorer along the repulsive wall and at longer range, since a spectroscopically determined potential does not accurately include the effects of van der Waals forces.

However, there is a long-range experimentally detected [26,41] local maximum in the potential for the $^1\Pi_u$ state of Na_2 that is reproduced by the theoretical calculations of Konowalow et al. [27] and by our HH potential obtained from the experimental spectroscopic constants [22,26], suggesting that the long-range representation by the HH potential might be quite accurate for the Na_2 potentials.

Figure 1 shows that the HH potential fit to the theoretical potential energy curve for the $^3\Sigma_u{}^+$ (2) state [28] and the exponential repulsive potential fit to the theoretical potential energy curve for the $^3\Pi_g$ state [27] are quite poor at larger interatomic separations. This should have little effect on the transport properties since, as discussed below, it is the inner wall of the potential, not the long-range tail, that makes the primary contribution to the transport properties especially at the higher temperatures at which these states contribute. The error in the fit for the $^3\Sigma_u{}^+$ (2) state has little effect on C_p^o since Table 2 shows that its contribution is negligible at all temperatures. In addition, the magnitude of $B_i(T)$ is small for this state compared with the value for a number of other states.

Another issue with the virial approach involves the sign of $B_i(T)$. The value of $B_i(T)$ for the $^3\Sigma_u{}^+$ (2) state of Na_2 becomes positive at about 1100 K, at about 1400 K for the $^3\Sigma_u{}^+$ (1) state, and at about 8000 K for the $^1\Sigma_g{}^+$ (2) state. Since [29]

$$B(T) = -K_c \tag{14}$$

where K_c is the equilibrium constant for the reaction,

$$Na + Na = Na_2 \tag{15}$$

then the result that $B_i(T) > 0$ is non-physical. However, this result is not surprising since the dissociation energies of these states are very small, and any molecules in these states would immediately dissociate at higher temperatures. In addition, the virial approach assumes that there is no interaction among various sodium clusters; e.g., Na, Na_2, Na_3, etc. [29]. Since the "true" interactions among clusters are likely to be attractive, the temperature at which $B_i(T)$ becomes positive would increase [40,42]. Table 2 shows that the contribution of the states with $B_i(T) > 0$ to the degeneracy-averaged virial coefficients is small at all temperatures, so that the "failure" of the formalism at higher temperatures for these states does not affect the calculated value of C_p^o.

Both approaches are less accurate at higher temperatures due to errors in Eq. 7 for the virial approach near the dissociation limit and due to errors in Eq. 10 for the state sum approach near the dissociation limit. However, the errors are likely to be less for the virial approach than for the state sum approach since excited states are accounted for in a more accurate way by the former approach and the latter approach does not include a contribution to C_p^o from continuum states.

Table 5 Viscosity collision integral, $\sigma^2\Omega^{(2,2)^*}$ (10^{-20} m^2), for each state as a function of temperature

State	500 K	10,000 K	20,000 K
$X\,^1\Sigma_g^+$ (1)	46.60	8.879	4.959
$^3\Sigma_u^+$ (1)	21.68	9.951	8.473
$^1\Sigma_u^+$	129.7	18.58	8.235
$^3\Sigma_g^+$	106.4	11.52	6.075
$^1\Sigma_g^+$ (2)	117.8	13.60	8.233
$^3\Pi_u$	82.95	14.90	6.588
$^1\Pi_u$	27.99	7.260	5.527
$^1\Pi_g$	85.71	7.339	5.172
$^3\Sigma_u^+$ (2)	14.23	6.183	5.072
$^3\Pi_g$	22.69	7.291	4.922

Table 3 shows the Boltzmann factors, $\exp(-E/kT)$, where E is the energy of the dissociated atoms, as a function of temperature. Dissociation to ^{1}S and ^{2}P atoms begins to become important at about 10,000 K and dissociation to two ^{2}P atoms begins to become important at about 20,000 K and should be included at higher temperatures.

The results for the transport properties in Table 4 are similar to those given in Table IV of Ref. [3] to 3000 K. At higher temperatures, the experimentally determined [23] HH potential for the $^3\Sigma_u^+$ (1) state, used for these calculations, gives different results for the viscosity collision integral than the theoretical HH potential [27] used in Ref. [3], and we include contributions from excited state atoms not included in Ref. [3]. Our viscosity collision integrals are thus larger than those given in Ref. [3], and the transport properties are smaller.

For the viscosity collision integrals, the contribution of all states is "similar", unlike for $B_i(T)$. Table 5 shows the viscosity collision integral for each state at several temperatures. The values differ by less than an order of magnitude at lower temperatures and by less than a factor of two at higher temperatures. However, the virial coefficients for the individual states differ by many orders of magnitude at 500 K and by about two orders of magnitude at higher temperatures.

The reason for this difference is that the collision integrals are determined primarily by the characteristics of the repulsive wall of the potential [43,44] which tend to be "similar" for different states so that $\Omega^{(2,2)^*}$ is similar for the various states. The primary difference is in the value of σ which ranges between 2.206×10^{-10} m and 4.246×10^{-10} m, a factor of less than 4. However, the virial coefficients are determined primarily by the well region of the potential [44,45]; D_e ranges from 3.461×10^{-21} J to 5.829×10^{-19} J, a factor of approximately 168. This is an important reason for the large difference in the values of the $B_i(T)$ for the various states.

Table VII of Ref. [3] compares the calculated and experimental [46–48] viscosities and thermal conductivities of sodium atoms. In general, the difference is no more than 15 %. The comparison with experiment is essentially unchanged for this work, since our transport property results and those in Ref. [3] are similar at lower temperatures. In addition, there is a rule-of-thumb [49,50] that an error of a factor of two in the

potential leads to an error of 20 % to 40 % in the transport collision integrals. We estimate the errors in the transport properties reported here to be no more than 20 % to about 15,000 K. Since, as for the C_p^o, contributions from collisions between two ^{2}P sodium atoms become important at about 20,000 K, the errors may be larger above 15,000 K.

The virial coefficients depend on the details of the potential in a more sensitive way than the transport properties. Thus, we estimate the errors in C_p^o at temperatures below 20,000 K to be 25 % or less.

References

1. B.M. Smirnov, M.I. Chibisov, High Temp. **9**, 467 (1971)
2. R.H. Davies, E.A. Mason, R.J. Munn, Phys. Fluids **8**, 444 (1965)
3. P.M. Holland, L. Biolsi, J. Chem. Phys. **87**, 1261 (1987)
4. O. Sinanoglu, K.S. Pitzer, J. Chem. Phys. **31**, 960 (1959)
5. F.H. Mies, P.S. Julienne, J. Chem. Phys. **77**, 6162 (1982)
6. M.W. Chase, Jr. (ed.), *NIST-JANAF Thermochemical Tables*, 4th edn., Part 2 (NIST, Washington, DC, 1998), p. 1647
7. G. Herzberg, *Molecular Spectra and Molecular Structure I. Spectra of Diatomic Molecules*, 2nd edn. (Van Nostrand, New York, 1950), pp. 318–321
8. D. Steele, E.R. Lippincott, J.T. Vanderslice, Rev. Mod. Phys. **34**, 239 (1962)
9. J.T. Vanderslice, E.A. Mason, W.G. Maisch, J. Chem. Phys. **32**, 515 (1960)
10. P.H. Krupenie, J. Phys. Chem. Ref. Data **1**, 423 (1972)
11. G.C. Lie, E. Clementi, J. Chem. Phys. **60**, 1288 (1974)
12. G. Das, A.C. Wahl, J. Chem. Phys. **44**, 87 (1966)
13. L. Biolsi, J.C. Rainwater, P.M. Holland, J. Chem. Phys. **77**, 448 (1982)
14. D. Klein, Z. Phys. **76**, 226 (1932)
15. R. Rydberg, Z. Phys. **80**, 514 (1933)
16. A.L.G. Rees, Proc. Phys. Soc. London **59**, 998 (1947)
17. J.C. Rainwater, P.M. Holland, L. Biolsi, Prog. Astronaut. Aeronaut. **82**, 3 (1982)
18. J.C. Rainwater, P.M. Holland, L. Biolsi, J. Chem. Phys. **77**, 434 (1982)
19. J.C. Rainwater, L. Biolsi, K.J. Biolsi, P.M. Holland, J. Chem. Phys. **79**, 1462 (1983)
20. H.M. Hulburt, J.O. Hirschfelder, J. Chem. Phys. **9**, 61 (1941)
21. H.M. Hulburt, J.O. Hirschfelder, J. Chem. Phys. **35**, 1901 (1961)
22. K.P. Huber, G. Herzberg, *Molecular Spectra and Molecular Structure IV. Constants of Diatomic Molecules* (Van Nostrand Reinhold, New York, 1979), pp. 432–433
23. L. Liu, S.F. Rice, R.W. Fields, J. Chem. Phys. **82**, 1178 (1985)
24. C. Effantin, O. Babaky, K. Hussein, J. d'Incan, R.F. Barrow, J. Phys. B **18**, 4077 (1985)
25. C. Effantin, J. d'Incan, A.J. Ross, R.F. Barrow, J. Verges, J. Phys. B **17**, 1515 (1984)
26. P. Kusch, M.M. Hessel, J. Chem. Phys. **68**, 2591 (1978)
27. D.D. Konowalow, M.E. Rosenkrantz, M.L. Olson, J. Chem. Phys. **72**, 2612 (1980)
28. G. Jeung, J. Phys. B **16**, 4289 (1983)
29. H.W. Woolley, J. Chem. Phys. **21**, 235 (1953)
30. W.G. Browne, Adv. Aero. Phys. Tech. Memo. No. 8 (GE Company, Valley Forge, PA, May 1962)
31. R. Phair, L. Biolsi, P.M. Holland, Int. J. Thermophys. **11**, 201 (1990)
32. J.O. Hirschfelder, C.F. Curtiss, R.B. Bird, *Molecular Theory of Gases and Liquids* (Wiley, New York, 1954) Chap. 8
33. M.E. Boyd, S.Y. Larsen, J.E. Kilpatrick, J. Chem. Phys. **50**, 4034 (1969)
34. L. Biolsi, P.M. Holland, Int. J. Thermophys. **17**, 191 (1996)
35. E.A. Mason, J.T. Vanderslice, Y.M. Yos, Phys. Fluids **2**, 688 (1959)
36. L. Biolsi, P.M. Holland, Int. J. Thermophys. **28**, 835 (2007)
37. L. Monchick, Phys. Fluids **2**, 695 (1959)
38. C.W. Beckett, L. Haar, in *Joint Conference on Thermodynamics and Transport Properties of Fluids*, ed. by O.A. Saunders (Inst. Mech. Eng., London, 1958), p. 27

39. G. Baumann, Z. Phys. Chem. **14**, 113 (1958)
40. M.L. Biolsi, L. Biolsi, P.M Holland, Paper # 368, American Chemical Society 228th National Meeting, Philadelphia, PA, Aug. 22–26, 2004
41. W. Demtroder, M. Stock, J. Mol. Spectrosc. **55**, 476 (1975)
42. E.A. Mason, T.H Spurling, in *International Encyclopedia of Physical Chemistry and Chemical Physics, Topic 10, The Fluid State, Vol. 2. The Virial Equation of State*, ed. by J.S. Rowlinson (Pergamon Press, Oxford, 1969), p. 61
43. L.A. Viehland, M.M. Harrington, E.A. Mason, Chem. Phys. **17**, 433 (1976)
44. A. Bousheri, L.A. Viehland, E.A. Mason, Physica **91A**, 424 (1978)
45. P. Clancy, D.W. Gough, G.P. Matthews, E.B. Smith, W.A. Wakeham, Mol. Phys. **30**, 1397 (1975)
46. D.L. Timrot, A.N. Varava, High Temp. **15**, 634 (1977)
47. N.V. Vargaftiak, A.A. Voschchinin, High Temp. **5**, 517 (1967)
48. D.L. Timrot, V.V. Makhrov, V.I. Sviridenko, High Temp. **14**, 58 (1976)
49. J.C. Rainwater, L. Biolsi, K.J. Biolsi, P.M. Holland, J. Chem. Phys. **79**, 1462 (1983)
50. P.H. Krupenie, E.A. Mason, J.T. Vanderslice, J. Chem. Phys. **39**, 2399 (1963)